Measurement and Feed Forward Induced Entanglement Negativity Transition

Alireza Seif,[1] Yu-Xin Wang (王语馨),[1,2] Ramis Movassagh,[3,4] and Aashish A. Clerk[1]
[1]Pritzker School of Molecular Engineering, University of Chicago, Chicago, Illinois 60637, USA
[2]Joint Center for Quantum Information and Computer Science, University of Maryland, College Park, Maryland 20742, USA
[3]IBM Quantum, MIT-IBM Watson AI Lab, Cambridge Massachusetts 02142, USA
[4]Google Quantum A.I., Venice, California 90291, USA

(Received 8 November 2023; revised 30 April 2024; accepted 25 June 2024; published 30 July 2024)

We study the interplay between measurement-induced dynamics and conditional unitary evolution in quantum systems. We numerically and analytically investigate commuting random measurement and feed forward (MFF) processes and find a sharp transition in their ability to generate entanglement negativity as the number of MFF channels varies. We also establish a direct connection between these findings and transitions induced by random dephasing from an environment with broken time-reversal symmetry. In one variant of the problem, we employ free probability theory to rigorously prove the transition's existence. Furthermore, these MFF processes have dynamic circuit representations that can be experimentally explored on current quantum computing platforms.

DOI: 10.1103/PhysRevLett.133.050402

The evolution of quantum systems is influenced differently by measurements versus unitary time evolution. Understanding the dynamics of entanglement under one or both of these two mechanisms is of interest from various perspectives. On one hand, the interplay between these processes can induce entanglement transitions in monitored quantum systems (see, e.g., Refs. [1–8]). On the other hand, incorporating measurements and adaptive operations into unitary circuits can facilitate the generation of long-range entangled and topologically ordered states, leveraging faster classical communication [9–17]. Note that studies of entanglement transitions typically focus on the system state conditioned on measurement outcomes, while in studies of adaptive dynamics, one deterministically prepares entangled states (with a final form that is not contingent on intermediate measurement results).

In this work, we explore a new question at the intersection of these two directions involving measurement-induced dynamics and conditional unitary evolution. Specifically, we investigate the interplay of multiple commuting random measurement and feed forward (MFF) channels. In our setting, individual random MFF channels are entangling, and as they commute, one might assume that this continues to be true even when they are combined. The reality is however more complex: we uncover a distinct transition in their ability to generate entanglement, characterized by negativity [18–20], as we vary the number of MFF channels. Our work stands apart from previous research on disordered open quantum systems, which has primarily focused on their spectral properties [21–23]. We instead unveil a scenario where this transition clearly emerges as a quantum characteristic of the dynamics.

We explore different variants of this general class of problems. Notably, in one variant, we analytically prove the existence of a sharp transition using tools from free probability. Additionally, these negativity transitions appear to be independent of local degrees of freedom and occur in both spin and bosonic systems. Our findings are also directly linked to a transition in the dynamics of a system coupled to a bath with broken time-reversal symmetry [24]. Our work represents one of the rare instances where exact descriptions of entanglement transitions are attainable [25].

We consider a system of n qubits undergoing continuous measurement and feed forward in the Markovian limit. As we explain below, the unconditional system evolution will follow a Gorini–Kossakowski–Sudarshan–Lindblad [26,27] equation, $\partial_t\hat{\rho} = \mathcal{L}[\hat{\rho}]$, where $\hat{\rho}$ is the system's state at time t and $\mathcal{L}$ is the generator of the dynamics.

First, let us examine the effect of weak continuous measurement of a Hermitian operator $\hat{A}_k$ on the system. Let $\alpha_k(t) = \langle \hat{A}_k \rangle + d\xi$ denote the stochastic continuous measurement record, where $d\xi$ is a Wiener increment [28]. The trajectories of the system, i.e., the state conditioned on $\alpha_k(t)$, could be entangled, as, in general, nonlocal measurements can generate entanglement [29–31]. However, this entanglement is contingent upon the outcome of the measurements; when the record is lost, the entanglement vanishes. Indeed, the dynamics of the unconditional state, i.e., the system's state averaged over the measurement outcomes, is generated by $\mathcal{L}[\hat{\rho}] = \mathcal{D}(\hat{A}_k)[\hat{\rho}]$, where

$$\mathcal{D}(\hat{A}_k)[\hat{\rho}] = \hat{A}_k\hat{\rho}\hat{A}_k^\dagger - \frac{1}{2}\{\hat{A}_k^\dagger\hat{A}_k, \hat{\rho}\}. \tag{1}$$

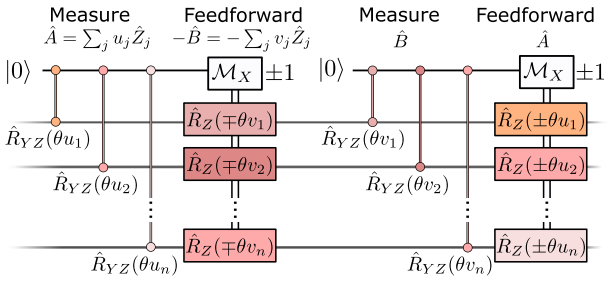

FIG. 1. Weak continuous measurements and feed forward of $\hat{A}$ and $\hat{B}$ in the Z basis. These operations can be implemented by repeated coupling to an auxiliary qubit with $\hat{R}_{YZ}$ rotations proportional to random u_j, measuring the qubit, and applying $\hat{R}_Z$ rotations proportional to random $-v_j$ whose sign is dictated by measurement results (± 1). Here, θ is a small parameter that determines the timescale. In the limit of small θ, repeated applications of this procedure together with the reverse direction $u_j \to v_j$ and $v_j \to -u_j$ realizes $\mathcal{D}(\hat{A} + i\hat{B})$ (3) [33,37].

In other words, the state is simply being dephased in the measurement basis.

Next, we add a feed forward Hamiltonian that takes the measurement signal and drives the system through $-\alpha_k(t)\hat{B}_k$, where $\hat{B}_k$ is some Hermitian system operator. This retains the information about the trajectories in the system and can preserve the entanglement in the unconditional state. As the delay between the measurement and feed forward operations approaches zero, the dynamics are governed by $\mathcal{L}[\rho] = -i[\hat{H}_k, \hat{\rho}] + \mathcal{D}(\hat{A}_k + i\hat{B}_k)[\rho]$, where $\hat{H}_k = \frac{1}{2}(\hat{A}_k\hat{B}_k + \hat{B}_k\hat{A}_k)$ [28,32,33].

This process can be represented by a dynamic quantum circuit [36], where the system is repeatedly and weakly coupled to an auxiliary qubit through $\hat{A}_k$, followed by the measurement of the auxiliary qubit with outcomes ± 1. Subsequently, depending on the outcome, we apply a small rotation around $\mp\hat{B}_k$ (see Fig. 1) [33,37].

In this work, we are interested in studying the simplest possible example of MFF dynamics that demonstrates a transition in entanglement properties of the system. Therefore, we choose commuting $\hat{A}_k$ and $\hat{B}_k$ that are all diagonal in the energy eigenbasis of the system (implying that the intrinsic system Hamiltonian plays no role). The dynamics might seem trivial with this choice, but as we show, this is surprisingly not the case. Moreover, to avoid breaking reciprocity, we choose bidirectional MFF processes. That is the only symmetry that we impose on the problem. Therefore, in addition to the weak measurement of $\hat{A}_k$ and driving the system through $-\alpha_k(t)\hat{B}_k$, we also apply the reverse scenario: measuring $\hat{B}_k$ and using the resulting record to apply a drive proportional to $\hat{A}_k$. As a result, the dynamics become fully dissipative with no Hamiltonian component. The directional case exhibits similar physics (see Ref. [33]).

We aim to explore the general characteristics of entanglement generation with multiple MFF channels. In particular, we are interested in whether the dynamics is entangling, i.e., if there exists some initial product state, such that the evolved state at some future time has nonzero entanglement negativity. Crucially, this entanglement can be transient and is not a steady-state property. Therefore, we consider the setup introduced earlier with m bidirectional random measurement and feed forward processes, where no additional structure is imposed beyond reciprocity. We then ask if the dynamics is entangling as we vary the system size n and the number of channels m. To keep the single qubit dephasing rates finite as we vary m and n, we normalize the MFF channels with system size. Specifically, we choose $\hat{A}_k = (1/\sqrt{n})\sum_j u_{jk}\hat{Z}_j$ and $\hat{B}_k = (1/\sqrt{n})\sum_j v_{jk}\hat{Z}_j$ for $k = 1, \ldots, m$, where $\hat{Z}_j$ is the Pauli $\hat{\sigma}_z$ operator on qubit j and v_{jk} and u_{jk} are chosen independently at random from a Gaussian distribution

$$v_{jk}, u_{jk} \sim \mathcal{N}(0, 1/2). \tag{2}$$

Each channel corresponds to measuring a weighted total spin along the z direction and applying single-qubit rotations proportional to the measurement signal, with different proportionality factors for each spin. The overall evolution induced by these m channels can be expressed as

$$\mathcal{L} = \sum_{k=1}^{m} \mathcal{D}(\hat{A}_k + i\hat{B}_k) = \sum_{k=1}^{m} \mathcal{D}\left(\frac{1}{\sqrt{n}}\sum_{j=1}^{n} w_{jk}\hat{Z}_j\right), \tag{3}$$

where $w_{jk} = u_{jk} + iv_{jk}$. We can equivalently represent the evolution as

$$\partial_t\hat{\rho} = \sum_{i,j=1}^{n} c_{ij}\left(\hat{Z}_i\hat{\rho}\hat{Z}_j - \frac{1}{2}\{\hat{Z}_j\hat{Z}_i, \hat{\rho}\}\right), \tag{4}$$

where $c_{ij} = (1/n)\sum_{k=1}^{m} w_{ik}\bar{w}_{jk}$. In matrix notation, this corresponds to $C = (1/n)WW^\dagger$, where $C = [c_{ij}] \in \mathbb{C}^{n\times n}$ and $W = [w_{ij}] \in \mathbb{C}^{n\times m}$. Thus the correlation between qubit dynamics introduced by various MFF processes can be inferred from C. The real part of C contributes to the decay of coherences (off-diagonal elements of $\hat{\rho}$), while the imaginary part, acting as dissipative Ising-like interactions, results in a phase evolution [24].

To quantify the entanglement, we employ entanglement negativity, which can be computed using the partial-transpose test [18–20]. In Ref. [24], it was demonstrated that we can assess the ability of the evolution described in Eq. (4) to generate bipartite entanglement negativity between a subsystem S and its complement by examining the spectrum of $\tilde{C}$ obtained from transforming C using the following rule:

$$\tilde{c}_{ij} = \begin{cases} -\mathrm{Re}(c_{ij}) & i \in S \text{ and } j \notin S \text{ (or vice versa)} \\ c_{ji} & i \in S \text{ and } j \in S \\ c_{ij} & \text{otherwise} \end{cases}. \quad (5)$$

The presence of negative eigenvalues in $\tilde{C}$'s spectrum signifies the capability of the evolution to generate entanglement in the system. This is because the generator of the evolution of the partial transposed state with respect to subsystem S has a similar form to Eq. (4) and is given by

$$\tilde{\mathcal{L}}_{\mathrm{diss}}(\hat{\rho}^{T_S}) = -i\left[\sum_{i,j} \tilde{h}_{ij}\hat{Z}_i\hat{Z}_j, \hat{\rho}^{T_S}\right] + \sum_{i,j} \tilde{c}_{ij}\left(\hat{Z}_i\hat{\rho}^{T_S}\hat{Z}_j - \frac{1}{2}\{\hat{Z}_i\hat{Z}_j, \hat{\rho}^{T_S}\}\right), \quad (6)$$

where $\tilde{h}_{ij} = \mathrm{Im}(C_{ij})$ for $i \in S$ and $j \notin S$. In other words, the dissipative Ising interaction $\mathrm{Im}(C_{ij})$ in our original master equation (4) plays the role of coherent interactions $\tilde{h}_{ij}$ in the partial-transposed frame. Since the coherent and dissipative parts commute in Eq. (6), we can treat the evolution generated by each independently. The former does not alter the spectrum of $\hat{\rho}^{T_S}$, while the latter is not necessarily completely positive, and a negative eigenvalue in $\tilde{C}$ indicates the presence of an initially unentangled state ($\hat{\rho}^{T_S} \geq 0$) that becomes entangled ($\hat{\rho}^{T_S} \not\geq 0$) under the evolution described by Eq. (4).

The problem of deciding the entangling power of random MFF channels then boils down to drawing random matrices $W \in \mathbb{C}^{n\times m}$ with varying n and m from a complex Ginibre ensemble [38], calculating $C = (1/n)WW^\dagger$, finding $\tilde{C}$ for a given bipartition, and examining $\lambda_{\min}(\tilde{C})$, the smallest eigenvalue of $\tilde{C}$. The sign of $\lambda_{\min}(\tilde{C})$ tells us about the entangling power of C. We remark that although our discussion here is focused on qubits, the results have broader applicability; for example, they extend directly to bosonic systems with commuting quadrature Lindblad operators [33]. Moreover, this transition in entangling power of C directly translates to a transition in the negativity of product quantum states orthogonal to the dephasing direction (e.g., $|+\rangle^{\otimes n}$ for qubits and vacuum for bosons) at a fixed time that has to be short (compared to dephasing rates) for qubits and can be arbitrarily long for bosons. This is because for bosons, entanglement can increase without bound as purity decreases [39]. In contrast, for qubits, entanglement is bounded, and below a certain purity level, mixed state negativity vanishes [33].

We first numerically study the entanglement negativity between one qubit and the rest of the system. Specifically, we examine the probability p of drawing an entangling sample [with $\lambda_{\min}(\tilde{C}) < 0$] from the ensemble described above as we vary $r = m/n$ [33]. For $m \ll n$, we expect to always have an entangling process ($p = 1$) as an individual

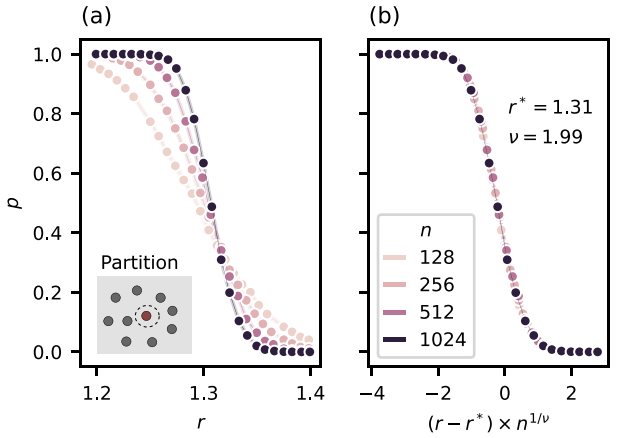

FIG. 2. (a) The fraction p of entangling samples, where each sample corresponds to a realization of m random measurement and feed forward channels in a system of n qubits, and we consider entanglement of one qubit with the remaining $n-1$ qubits. For large n, p undergoes a sharp transition as a function of $r = m/n$. (b) The critical point r^* and the correlation critical exponent ν are obtained using data collapse.

MFF channel in isolation will in general be entangling [24], and there is a negligible chance for different channels to overlap with each other. However, in the opposite limit of $m \gg n$, different MFF channels start to overlap, and hence the resulting correlations generated by these processes average away. This leads to $C \propto I$, implying that the net evolution is equivalent to driving with uncorrelated classical noise, which does not generate entanglement ($p = 0$). Therefore, we expect a crossover in p from 0 to 1 as we vary r from 0 to ∞. Surprisingly, however, we observe that p goes through a sharp transition from 1 to 0 when $r^* \approx 1.3$, i.e., when the number of MFF channels becomes comparable to system size [see Fig. 2(a)]. We also obtain the critical exponent of $\nu \approx 2$, by collapsing the data using the scaling form $p = f[(r - r^*)n^{1/\nu}]$ [see Fig. 2(b)].

Additionally, we analyze the transition using perturbation theory. Let $K = C - \tilde{C}$, where $\tilde{C}$ is obtained from Eq. (5). Therefore, the transformation to the partial-transposed frame of Eq. (6) can be interpreted as adding a perturbation K to the original coefficients C, that is

$$\tilde{C} = C + K. \quad (7)$$

We focus on the asymptotic regime of $n \to \infty$. In this limit, the spectrum of C follows the Marchenko-Pastur distribution [40]

$$d\mu(\lambda) = \max[0, (1-r)]\delta_0 + \frac{\sqrt{(b-\lambda)(\lambda-a)}}{2\pi\lambda}\mathbf{1}_{[a,b]}d\lambda, \quad (8)$$

where $a = (1-\sqrt{r})^2$ and $b = (1+\sqrt{r})^2$. Additionally, K is a rank-2 matrix with eigenvalues $\pm\kappa$, whose magnitude concentrates at $\kappa = \sqrt{r/2}$ [33].

When $r \ll 1$, C is a low-rank matrix with many 0 eigenvalues. Using degenerate perturbation theory [41], we show that K splits these eigenvalues and $\lambda_{\min}(\tilde{C}) < 0$. Degenerate perturbation theory is valid as long as the size of the perturbation ($\sqrt{r/2}$) is smaller than the spacing separating the degenerate subspace from the rest of the spectrum [$(1-\sqrt{r})^2$]. Therefore, we have $p = 1$ when $\sqrt{r/2} < (1-\sqrt{r})^2$, or equivalently when $r \lessapprox 0.2$.

In the limit of $r \gg 1$, the perturbation is small compared to $\lambda_{\min}(C) = (1-\sqrt{r})^2$, and therefore cannot change its sign. Specifically, using Weyl's inequality [42] we have

$$\lambda_{\min}(C) + \lambda_{\min}(K) \leq \lambda_{\min}(\tilde{C}). \tag{9}$$

Therefore, when $(1-\sqrt{r})^2 - \sqrt{r/2} > 0$, or equivalently when $r \gtrapprox 5.1$, we have $\lambda_{\min}(\tilde{C}) > 0$ and consequently $p = 0$.

The constant values of $p = 0$ and $p = 1$ within these nonvanishing intervals indicate the nonanalytic behavior of p as $n \to \infty$. This highlights the critical nature of the observed transition in negativity.

To go beyond the perturbative treatment and gain a deeper understanding, we must determine the eigenvalues of $\tilde{C}$ in Eq. (7). However, computing the eigenvalues of the sum of two matrices is a highly challenging problem that has long captivated mathematicians [43]. Finding exact solutions to this problem is generally difficult, except in special cases. One remarkable case is that of independent random matrices. In our problem, however, the matrices K and C in Eq. (7) are not independent. Nevertheless, we find a slightly different but related physical process by modifying our original problem that allows us to rigorously understand the transition.

Specifically, we introduce K' as a replacement for K, where the elements of K' have the same distribution as K but are now independent of C. Consequently, we focus on the alternative problem of finding the smallest eigenvalue of $\tilde{C}' = C + K'$. While this may seem arbitrary and disconnected from the original problem, the assumption of independence has an intriguing physical interpretation: it corresponds to a scenario where, in addition to the dissipative evolution given by Eq. (4), there is an Ising ZZ Hamiltonian [see Fig. 3(a)] whose coefficients are correlated with the dissipation, given by

$$\hat{H}_{ZZ} = \sum_j [k'_{1j} - \mathrm{Im}(c_{1j})]\hat{Z}_1\hat{Z}_j. \tag{10}$$

This Hamiltonian is entangling. Hence, we expect it to shift the critical point to the right as now there is an additional process contributing to the entanglement generation. This observation is supported by numerical experiments and the following analytical treatment [see Fig. 3(b)].

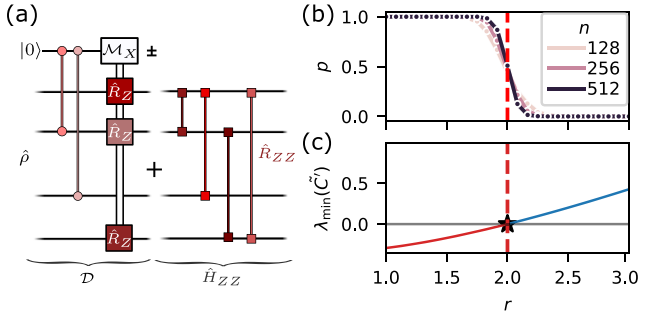

FIG. 3. (a) Circuit realization of our modified dynamics, where an additional Ising interaction Hamiltonian $\hat{H}_{ZZ}$ is combined with the MFF channels of the original setup. $\hat{H}_{ZZ}$ is random but in a way that is correlated with the MFF channels. This problem has an analytically proven transition. (b) Numerical simulation shows that the transition point is shifted to $r^* = 2$. (c) Analytical calculations of $\lambda_{\min}(\tilde{C}')$ show that its sign changes (and hence the transition happens) at $r^* = 2$.

To find the spectrum of $\tilde{C}'$ in the large n limit, we use the results of Ref. [44] regarding the eigenvalues of low-rank perturbations to large random matrices. The rotational invariance of the eigenvectors of C allows us to find a simple expression for the eigenvalues of $C + \tilde{K}'$. In particular, we find that for $r > 2(3+2\sqrt{2})$ the spectrum of C and $\tilde{C}'$ coincide and the perturbation $\tilde{K}'$ does not affect the minimal eigenvalue [$(1-\sqrt{r})^2$], which is consistent with our perturbative analysis [33]. However, for $1 < r < 2(3+2\sqrt{2})$ the perturbation modifies the spectrum of C. In this regime, the minimal eigenvalue of $\tilde{C}'$ is instead given by

$$\lambda_{\min}(\tilde{C}') = G^{-1}\left(\frac{-1}{\sqrt{r/2}}\right) = r - \frac{3}{\sqrt{2}}\sqrt{r} - \frac{4}{\sqrt{2r}+2} + 2, \tag{11}$$

where $G(z) = \int_{\mathbb{R}} 1/(z-t)d\mu(t)$ is the Cauchy transform of the measure μ [45]. Consequently, we can see that $\lambda_{\min}(\tilde{C}') < 0$ for $1 < r < 2$, and is non-negative for $r \geq 2$. Hence, $r^* = 2$ is the transition point for the entanglement generation in this model [see Figs. 3(b) and 3(c)] [33]. Moreover, using numerical simulations we find that in the modified model $\nu = 1.9$ consistent with the original model [33]. While we considered the entanglement negativity of 1 and $n-1$ qubit subsystems here, this analysis can be carried to other finite bipartitions.

The correlated dephasing process in the original model of Eq. (4) has several interpretations. So far, we have been interpreting it as the dynamics generated by MFF channels. Alternatively, it could correspond to a general dephasing environment with broken time-reversal symmetry (TRS) [24]. Therefore, the question of the entangling power of random MFF channels can be rephrased as a quantum-to-classical transition: can a random structureless quantum bath with broken TRS generate entanglement, or does it fail

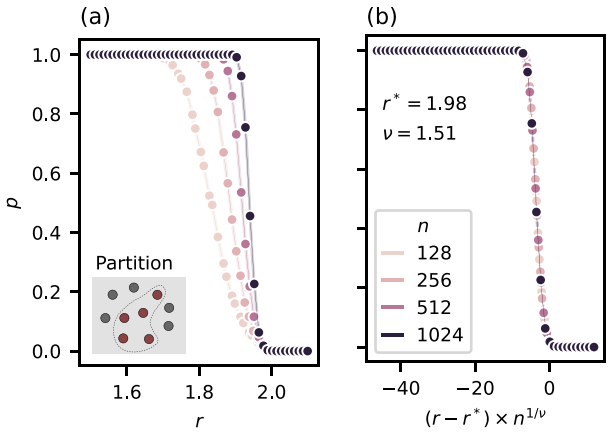

FIG. 4. (a) Entanglement transition similar to Fig. 2 for a half system partition. (b) The data collapses with a modified critical point r^* and exponent ν. The shift of the critical point indicates the more robust entanglement in this bipartition.

to generate entanglement and, in turn, appear as a classical environment from the system's perspective? To answer the question about the nature of the environment, we need to check the entangling power for all bipartitions. As we change the size of two partitions from 1 and $n-1$ to $n/2$ and $n/2$ the critical point shifts to the right, i.e., the entanglement is more robust for the half-system bipartition. We repeat the numerical analysis for this case and observe that the sharp transition persists although with shifted $r^* \approx 2$ and $\nu \approx 1.5$; see Fig. 4.

The observation that r^* remains a constant near 1, even as the partitions become extensive with the system size, suggests that when the number of dephasing channels in the environment becomes comparable to the system size, the system effectively perceives the environment as classical. Thus, even though individual environment channels may possess quantum characteristics, their collective impact does not have any discernible quantum effect on the system. This phenomenon exemplifies a quantum-to-classical transition, where the increasing size of the environment leads to an effective classical behavior. Incorporating feed forward into measurement dynamics unveils an intriguing feature in the average postmeasurement state of the system, allowing it to retain entanglement generated by measurements. As more MFF channels are introduced, the entangling power of this evolution undergoes a sharp transition. This transition can also be seen as a transition in the nature of the environment as perceived by the system. Remarkably, the existence of this transition is not limited to spin systems, but is, in fact, independent of local degrees of freedom; for example, we observe an analogous transition in bosonic systems with similar kinds of dynamics [33].

The MFF channels we discuss in this work can be represented by circuits that are practical for implementation in currently available quantum computers [46–48]. Quantum simulations of this entangling transition can shed light on the dynamic interplay between these engineered MFF channels and the inherent noise within the quantum device.

While our study primarily focused on a specific class of random commuting MFF channels, exploring more general cases involving noncommuting MFF channels could yield interesting insights. Additionally, investigating the scaling of entanglement in scenarios with local or sparse interactions (in contrast to the all-to-all connectivity considered in this work) represents a promising avenue for future research.

Acknowledgements—We thank Tomaz Prosen, Michael Gullans, Yi-Kai Liu, Ali Lavasani, and Tarun Grover for helpful discussions. This work was supported by the Air Force Office of Scientific Research MURI program under Grant No. FA9550-19-1-0399, and the Simons Foundation through a Simons Investigator award (Grant No. 669487). A. S. was partially supported by a Chicago Prize Postdoctoral Fellowship in Theoretical Quantum Science.

[1] M. P. Fisher, V. Khemani, A. Nahum, and S. Vijay, Random quantum circuits, Annu. Rev. Condens. Matter Phys. **14**, 335 (2023).
[2] M. J. Gullans and D. A. Huse, Scalable probes of measurement-induced criticality, Phys. Rev. Lett. **125**, 070606 (2020).
[3] M. Ippoliti and V. Khemani, Postselection-free entanglement dynamics via spacetime duality, Phys. Rev. Lett. **126**, 060501 (2021).
[4] J. C. Hoke, M. Ippoliti, D. Abanin, R. Acharya, M. Ansmann, F. Arute, K. Arya, A. Asfaw, J. Atalaya, J. C. Bardin *et al.*, Measurement-induced entanglement and teleportation on a noisy quantum processor, Nature (London) **622**, 481 (2023).
[5] Y. Li, Y. Zou, P. Glorioso, E. Altman, and M. P. A. Fisher, Cross entropy benchmark for measurement-induced phase transitions, Phys. Rev. Lett. **130**, 220404 (2023).
[6] A. J. Friedman, O. Hart, and R. Nandkishore, Measurement-induced phases of matter require feedback, PRX Quantum **4**, 040309 (2023).
[7] Y. Bao, S. Choi, and E. Altman, Theory of the phase transition in random unitary circuits with measurements, Phys. Rev. B **101**, 104301 (2020).
[8] M. Buchhold, T. Müller, and S. Diehl, Revealing measurement-induced phase transitions by pre-selection, arXiv:2208.10506.
[9] E. Dennis, A. Kitaev, A. Landahl, and J. Preskill, Topological quantum memory, J. Math. Phys. (N.Y.) **43**, 4452 (2002).
[10] L. Piroli, G. Styliaris, and J. I. Cirac, Quantum circuits assisted by local operations and classical communication: Transformations and phases of matter, Phys. Rev. Lett. **127**, 220503 (2021).
[11] T.-C. Lu, L. A. Lessa, I. H. Kim, and T. H. Hsieh, Measurement as a shortcut to long-range entangled quantum matter, PRX Quantum **3**, 040337 (2022).

[12] R. Verresen, N. Tantivasadakarn, and A. Vishwanath, Efficiently preparing Schrödinger's cat, fractons and non-Abelian topological order in quantum devices, arXiv:2112.03061.
[13] N. Tantivasadakarn, R. Thorngren, A. Vishwanath, and R. Verresen, Long-range entanglement from measuring symmetry-protected topological phases, Phys. Rev. X **14**, 021040 (2024).
[14] N. Tantivasadakarn, R. Verresen, and A. Vishwanath, Shortest route to non-Abelian topological order on a quantum processor, Phys. Rev. Lett. **131**, 060405 (2023).
[15] N. Tantivasadakarn, A. Vishwanath, and R. Verresen, Hierarchy of topological order from finite-depth unitaries, measurement, and feed forward, PRX Quantum **4**, 020339 (2023).
[16] S. Bravyi, I. Kim, A. Kliesch, and R. Koenig, Adaptive constant-depth circuits for manipulating non-Abelian anyons, arXiv:2205.01933.
[17] T.-C. Lu, Z. Zhang, S. Vijay, and T. H. Hsieh, Mixed-state long-range order and criticality from measurement and feedback, PRX Quantum **4**, 030318 (2023).
[18] A. Peres, Separability criterion for density matrices, Phys. Rev. Lett. **77**, 1413 (1996).
[19] M. Horodecki, P. Horodecki, and R. Horodecki, Mixed-state entanglement and distillation: Is there a "bound" entanglement in nature?, Phys. Rev. Lett. **80**, 5239 (1998).
[20] M. Horodecki, P. Horodecki, and R. Horodecki, Separability of n-particle mixed states: Necessary and sufficient conditions in terms of linear maps, Phys. Lett. A **283**, 1 (2001).
[21] L. Sá, P. Ribeiro, and T. Prosen, Spectral and steady-state properties of random Liouvillians, J. Phys. A **53**, 305303 (2020).
[22] T. Can, V. Oganesyan, D. Orgad, and S. Gopalakrishnan, Spectral gaps and midgap states in random quantum master equations, Phys. Rev. Lett. **123**, 234103 (2019).
[23] K. Wang, F. Piazza, and D. J. Luitz, Hierarchy of relaxation timescales in local random Liouvillians, Phys. Rev. Lett. **124**, 100604 (2020).
[24] A. Seif, Y.-X. Wang, and A. A. Clerk, Distinguishing between quantum and classical Markovian dephasing dissipation, Phys. Rev. Lett. **128**, 070402 (2022).
[25] X. Feng, B. Skinner, and A. Nahum, Measurement-induced phase transitions on dynamical quantum trees, PRX Quantum **4**, 030333 (2023).
[26] V. Gorini, A. Kossakowski, and E. C. G. Sudarshan, Completely positive dynamical semigroups of n-level systems, J. Math. Phys. (N.Y.) **17**, 821 (1976).
[27] G. Lindblad, On the generators of quantum dynamical semigroups, Commun. Math. Phys. **48**, 119 (1976).
[28] H. M. Wiseman and G. J. Milburn, *Quantum Measurement and Control* (Cambridge University Press, Cambridge, England, 2009), 10.1017/CBO9780511813948.
[29] M. Van Regemortel, Z.-P. Cian, A. Seif, H. Dehghani, and M. Hafezi, Entanglement entropy scaling transition under competing monitoring protocols, Phys. Rev. Lett. **126**, 123604 (2021).
[30] A. Lavasani, Z.-X. Luo, and S. Vijay, Monitored quantum dynamics and the Kitaev spin liquid, Phys. Rev. B **108**, 115135 (2023).
[31] A. Sriram, T. Rakovszky, V. Khemani, and M. Ippoliti, Topology, criticality, and dynamically generated qubits in a stochastic measurement-only Kitaev model, Phys. Rev. B **108**, 094304 (2023).
[32] A. Metelmann and A. A. Clerk, Nonreciprocal quantum interactions and devices via autonomous feed forward, Phys. Rev. A **95**, 013837 (2017).
[33] See Supplemental Material at http://link.aps.org/supplemental/10.1103/PhysRevLett.133.050402 for details of perturbative and analytical calculations, circuit models of MFF dynamics, and the extension of the results to directional MFF channels and bosonic systems, which includes Refs. [34,35].
[34] Y. Wang, Noise and fluctuations for quantum information processing, Ph.D. thesis, The University of Chicago, 2023.
[35] C. Weedbrook, S. Pirandola, R. García-Patrón, N. J. Cerf, T. C. Ralph, J. H. Shapiro, and S. Lloyd, Gaussian quantum information, Rev. Mod. Phys. **84**, 621 (2012).
[36] Get started with dynamic circuits, https://docs.quantum-computing.ibm.com/build/getting-started-with-dynamic-circuits, accessed: 2023-10-25.
[37] J. A. Gross, C. M. Caves, G. J. Milburn, and J. Combes, Qubit models of weak continuous measurements: Markovian conditional and open-system dynamics, Quantum Sci. Technol. **3**, 024005 (2018).
[38] J. Ginibre, Statistical ensembles of complex, quaternion, and real matrices, J. Math. Phys. (N.Y.) **6**, 440 (1965).
[39] Y.-X. Wang, A. Seif, and A. A. Clerk, Uncovering measurement-induced entanglement via directional adaptive dynamics and incomplete information, arXiv:2310.01338.
[40] V. A. Marchenko and L. A. Pastur, Distribution of eigenvalues for some sets of random matrices, Mat. Sb. **114**, 507 (1967).
[41] J. Sakurai and J. Napolitano, *Modern Quantum Mechanics*, 2nd ed. Person New International edition 35 (Cambridge University Press, Cambridge, 2014).
[42] H. Weyl, Das asymptotische verteilungsgesetz der eigenwerte linearer partieller differentialgleichungen (mit einer anwendung auf die theorie der hohlraumstrahlung), Math. Ann. **71**, 441 (1912).
[43] A. Knutson and T. Tao, Honeycombs and sums of Hermitian matrices, Not. Am. Math. Soc. **48**, 175 (2001).
[44] F. Benaych-Georges and R. R. Nadakuditi, The eigenvalues and eigenvectors of finite, low rank perturbations of large random matrices, Adv. Math. **227**, 494 (2011).
[45] J. A. Mingo and R. Speicher, *Free Probability and Random Matrices* (Springer, New York, 2017), Vol. 35.
[46] E. Bäumer, V. Tripathi, D. S. Wang, P. Rall, E. H. Chen, S. Majumder, A. Seif, and Z. K. Minev, Efficient long-range entanglement using dynamic circuits, arXiv:2308.13065.
[47] M. Iqbal, N. Tantivasadakarn, T. M. Gatterman, J. A. Gerber, K. Gilmore, D. Gresh, A. Hankin, N. Hewitt, C. V. Horst, M. Matheny *et al.*, Topological order from measurements and feed-forward on a trapped ion quantum computer, arXiv:2302.01917.
[48] M. Foss-Feig, A. Tikku, T.-C. Lu, K. Mayer, M. Iqbal, T. M. Gatterman, J. A. Gerber, K. Gilmore, D. Gresh, A. Hankin *et al.*, Experimental demonstration of the advantage of adaptive quantum circuits, arXiv:2302.03029.